Modelling magnetic fields and turbulence with SPH

Daniel J. Price
Monash Centre for Astrophysics (MoCA)
and School of Mathematical Sciences
Monash University, Vic. 3800, Australia
daniel.price@monash.edu

***Abstract*—In recent years several key advances have been made in modelling both magnetic fields and turbulence in smoothed particle hydrodynamics. Solving the equations of magnetohydrodynamics (MHD) has proved an ongoing challenge over the last 35 years, but we have recently made a key breakthrough by developing a robust and safe method for enforcing the divergence-free condition on the magnetic field, enabling smoothed particle magnetohydrodynamics simulations with control of divergence errors and no restrictions on the field geometry. Modelling turbulence in SPH has benefited from faster algorithms allowing high resolution calculations capable of resolving the inertial range, particularly in supersonic flow, though SPH is most efficient when studying statistics of the density field, such as the density PDF. In subsonic flow use of viscosity switches is key to reaching high Reynolds numbers, which has been the source of recent controversy.**

I. Introduction

Magnetic fields and turbulence are important physical processes not only in many areas of astrophysics but also in Earth-bound applications of smoothed particle hydrodynamics (SPH). Both of these processes are thought to play a key role during the formation of stars from the gravitational collapse of interstellar clouds [17], a problem that SPH was originally designed for [10], [16] and is very well suited to modelling because of the ability to adaptively resolve the many orders of magnitude change in length and timescales involved. Turbulence itself is a ubiquitous phenomenon that defies analytic solution, so from the outset requires a numerical approach in order to model any system it occurs in. Recently we have made great strides in modelling both magnetic fields and turbulence using SPH, both of which I will attempt to outline in this paper.

II. Magnetic fields

A. Magnetohydrodynamics

Magnetic fields are usually modelled in the magnetohydrodynamics (MHD) approximation, where the equations of fluid dynamics adopt the form

$$\frac{\mathrm{d}\rho}{\mathrm{d}t} = -\rho\nabla\cdot\mathbf{v}, \quad (1)$$

$$\frac{\mathrm{d}\mathbf{v}}{\mathrm{d}t} = -\frac{1}{\rho}\nabla\cdot\left[\left(P+\frac{1}{2}\frac{B^2}{\mu_0}\right)I-\frac{\mathbf{BB}}{\mu_0}\right], \quad (2)$$

$$\frac{\mathrm{d}u}{\mathrm{d}t} = -\frac{P}{\rho}\nabla\cdot\mathbf{v}, \quad (3)$$

$$\frac{\mathrm{d}\mathbf{B}}{\mathrm{d}t} = (\mathbf{B}\cdot\nabla)\mathbf{v}-\mathbf{B}(\nabla\cdot\mathbf{v}), \quad (4)$$

where ρ is the density, $\mathbf{v}$ is the velocity, P is the gas pressure, u is the specific thermal energy, $\mathbf{B}$ is the magnetic field, infinite electrical conductivity has been assumed, $\mathrm{d}/\mathrm{d}t \equiv \partial/\partial t + (\mathbf{v}\cdot\nabla)$ refers to the comoving (Lagrangian) derivative, and the equation set is closed by adopting an appropriate equation of state (e.g. $P=(\gamma-1)\rho u$).

B. Smoothed Particle Magnetohydrodynamics

Although an early attempt was made by Gingold & Monaghan [10] to model magnetic stars, Phillips and Monaghan [25] represented the first systematic attempt to formulate the MHD equations in SPH, later coined 'Smoothed Particle Magnetohydrodynamics' (SPMHD) by Joe Morris [22]. In their most basic form the equations are very similar to the usual SPH equations and, like the SPMHD equations, can be derived in a self-consistent manner using a variational principle [37]. Taking full account of a spatially variable smoothing length h, the equations on a given particle a are given by

$$\rho_a = \sum_b m_b W_{ab}(h_a), \quad (5)$$

$$\frac{\mathrm{d}v_a^i}{\mathrm{d}t} = \sum_b m_b\left[\frac{S_a^{ij}}{\Omega_a\rho_a^2}\frac{\partial W_{ab}(h_a)}{\partial x_a^j}+\frac{S_b^{ij}}{\Omega_b\rho_b^2}\frac{\partial W_{ab}(h_b)}{\partial x_a^j}\right], \quad (6)$$

$$\frac{\mathrm{d}u_a}{\mathrm{d}t} = \frac{P_a}{\Omega_a\rho_a^2}\sum_b m_b(\mathbf{v}_a-\mathbf{v}_b)\cdot\nabla W_{ab}(h_a), \quad (7)$$

where the summations are over neighbouring particles, $b = 1..N_{\mathrm{neigh}}$, within the kernel radius, the MHD stress tensor is defined according to

$$S^{ij} \equiv -\left(P+\frac{1}{2}\frac{B^2}{\mu_0}\right)\delta^{ij}+\frac{B^iB^j}{\mu_0}, \quad (8)$$

and Ω is a dimensionless correction term resulting from the smoothing length gradients (see [19], [39]).

C. Removing the tensile instability in SPMHD

Phillips and Monaghan [25] discovered that the momentum-conserving formulation of the equations of motion (Eq. 6) is unstable when the magnetic pressure exceeds the gas pressure, $\frac{1}{2}B^2/\mu_0 > P$. The reason for this is both numerical and physical. The numerical explanation is that in this regime the overall stress tensor is negative, resulting in a negative total pressure, which when combined with the negative-definite sign of the kernel gradient in Eq. 6, results in an attractive

force between particles along magnetic field lines that causes them to catastrophically clump together (see [31] for a more detailed explanation). The physical reason that this occurs in MHD is related to the presence of magnetic monopole ($\nabla \cdot \mathbf{B}$) terms when the equations of motion for MHD are written in a conservative form. That is, Eq. 2 can be expanded to give

$$\frac{\mathrm{d}\mathbf{v}}{\mathrm{d}t} = -\frac{\nabla P}{\rho} + \frac{\mathbf{J}\times\mathbf{B}}{\rho} + \frac{\mathbf{B}\nabla\cdot\mathbf{B}}{\mu_0\rho}, \tag{9}$$

which contains both the physical Lorentz force (where $\mathbf{J} = (\nabla\times\mathbf{B})/\mu_0$ is the current density) and an *unphysical* term proportional to the divergence of the magnetic field. This 'monopole force' is attractive and directed along magnetic field lines, is inevitably present in SPMHD when Eq. 6 is employed, and is the physical source of the tensile instability in Lagrangian MHD codes. Thus, the best way to remove the tensile instability in SPMHD is to explicitly subtract this term, as proposed by [3], [4] by adding a corrective 'source term' to Eq. 6 of the form

$$\left(\frac{\mathrm{d}\mathbf{v}}{\mathrm{d}t}\right)_{\mathrm{corr}} = -\frac{\mathbf{B}\nabla\cdot\mathbf{B}}{\mu_0\rho}, \tag{10}$$

where the key is to discretise $\nabla\cdot\mathbf{B}$ *in the form that it is used in the momentum equation*, i.e., using the symmetric SPH representation of a first derivative, which in the variable smoothing length formulation of SPH is given by (e.g. [29], [31])

$$\frac{\nabla\cdot\mathbf{B}}{\rho_a} = \sum_b m_b\left[\frac{B_a^j}{\Omega_a\rho_a^2}\frac{\partial W_{ab}(h_a)}{\partial x_a^j} + \frac{B_b^j}{\Omega_b\rho_b^2}\frac{\partial W_{ab}(h_b)}{\partial x_a^j}\right], \tag{11}$$

With the correction applied in this form, the tensile instability issue is resolved in SPMHD, with the trade-off being that momentum is no longer exactly conserved to the extent to which $\nabla\cdot\mathbf{B}$, discretised via Eq. (11) is non-zero. With the correction term subtracted, the anisotropic part of the force (that which produces tension perpendicular to magnetic field lines) becomes

$$\left(\frac{\mathrm{d}v_a^i}{\mathrm{d}t}\right)_{aniso} = \sum_b m_b\left[\frac{B_a^iB_a^j - B_b^iB_b^j}{\Omega_b\rho_b^2}\right]\frac{\partial W_{ab}(h_b)}{\partial x_a^j}, \tag{12}$$

which is in the end very similar to the modified anisotropic force proposed by Morris [22] to remove the SPMHD tensile instability. This explains why the 'Morris approach' and the 'source term approach' give essentially indistinguishable results on test problems (c.f. [27], [31]).

D. Dissipation terms in SPMHD

The second issue, first considered by [36], was to formulate artificial dissipation terms for SPMHD, generalising the artificial viscosity terms used for purely hydrodynamic simulations. The main requirement for MHD is the addition of an artificial resistivity term in the induction equation in order to deal with discontinuities in the magnetic field, in the form

$$\left(\frac{d\mathbf{B}_a}{dt}\right)_{diss} = \rho_a\sum_b m_b\frac{\alpha_B v_{sig}^B}{\bar{\rho}_{ab}^2}\left(\mathbf{B}_a - \mathbf{B}_b\right)\bar{F}_{ab}, \tag{13}$$

where

$$v_{sig}^B = \frac{1}{2}\sqrt{v_{A,a}^2 + v_{A,b}^2}; \qquad v_A^2 = \frac{B^2}{\mu_0\rho}. \tag{14}$$

and where α_B can be evolved using a switch similar to that proposed by [23], with [38] suggesting a source term that responds to magnetic discontinuities of the form

$$\mathcal{S} = \max\left(\frac{|\nabla\times\mathbf{B}|}{\sqrt{\mu_0\rho}}, \frac{|\nabla\cdot\mathbf{B}|}{\sqrt{\mu_0\rho}}\right). \tag{15}$$

The corresponding term in the thermal energy equation, as well as the usual artificial viscosity and artificial conductivity terms for dealing with the hydrodynamic discontinuities (shocks and contact discontinuities, respectively) are given in [38] and [31].

E. The divergence constraint in SPMHD

The third and most difficult issue, is how to enforce the $\nabla\cdot\mathbf{B} = 0$ 'no monopoles' constraint in the SPMHD evolution of the MHD equations. Although one of Maxwell's equations, the constraint only enters the MHD equations implicitly as an initial condition. That is, taking the divergence of the induction equation in the form

$$\frac{\partial\mathbf{B}}{\partial t} = \nabla\times(\mathbf{v}\times\mathbf{B}), \tag{16}$$

gives

$$\frac{\partial}{\partial t}(\nabla\cdot\mathbf{B}) = 0, \tag{17}$$

implying that, if the divergence of the magnetic field is initially zero, it should remain so for all time. However, this will clearly not remain true in any numerical code.

1) Source term approach: The 0th order approach is to ensure that any divergence errors, though present, do not grow. This is the essence of Powell et al.'s 'source term approach' [26], where the induction equation is modified by subtracting the divergence term, i.e.

$$\frac{\partial\mathbf{B}}{\partial t} = \nabla\times(\mathbf{v}\times\mathbf{B}) - \mathbf{v}(\nabla\cdot\mathbf{B}), \tag{18}$$

which, when expanded out and written with the Lagrangian time derivative, is identical to our Eq. 4. With this formulation, divergence errors evolve according to

$$\frac{\partial}{\partial t}(\nabla\cdot\mathbf{B}) + \nabla\cdot(\mathbf{v}\nabla\cdot\mathbf{B}) = 0, \tag{19}$$

which is similar to the continuity equation (Eq. 1) but for the monopole density $\rho_m \equiv \nabla\cdot\mathbf{B}$. This implies monopoles are 'conserved' by the flow, and furthermore that magnetic flux through surfaces is conserved even in the presence of non-zero divergence errors, since

$$\frac{\mathrm{d}}{\mathrm{d}t}\int(\nabla\cdot\mathbf{B})\mathrm{d}V = \frac{\mathrm{d}}{\mathrm{d}t}\oint\mathbf{B}\cdot\mathrm{d}\mathbf{S} = 0. \tag{20}$$

Powell et al. also proposed subtracting a source term from the momentum equation, identical to that which we have already subtracted in SPMHD to remove the tensile instability (see above).

However, the source term approach proves insufficient for the long term evolution of dynamic, 3D problems such as star formation, where the non-conservation of momentum that results from subtracting a large divergence error can result in severe numerical problems, such as stars that 'explode' rather than collapse under gravity.

2) Failure of cleaning and use of the Euler potentials: Price & Monaghan [38] investigated various approaches to 'cleaning' the divergence error in SPMHD, including elliptic projection methods (based on an approach similar to that used for solving for the gravitational field) and the hyperbolic/parabolic cleaning proposed by Dedner et al. [8]. While reasonable results were found on simple test problems, none of these methods was later found to perform sufficiently well on realistic, 3D problems. For this reason [32] and [41] turned to the 'Euler potentials' formulation initially considered by [25], where the magnetic field is written in the form

$$\mathbf{B} = \nabla\alpha \times \nabla\beta, \tag{21}$$

with the advantage that the induction equation (Eq. 4) adopts the trivial form

$$\frac{\mathrm{d}\alpha}{\mathrm{d}t} = 0; \quad \frac{\mathrm{d}\beta}{\mathrm{d}t} = 0, \tag{22}$$

corresponding physically to the advection of magnetic field lines by Lagrangian particles [42]. Using Eq. 21 the divergence constraint is satisfied by construction (meaning in practice to truncation error once the gradient operators are represented by their SPMHD equivalents). This means that 'exploding stars' and the like do not occur, and as a result this formulation was successfully applied to several problems in star formation (e.g. [32], [33]) and elsewhere (e.g. [13]). However, the formulation via Euler potentials is overly restrictive, limiting the geometry of the field to topologically simple forms, excluding from the outset any dynamo processes and preventing the inclusion of non-ideal MHD effects such as resistivity in a self-consistent manner [5]. This means that it is useful only for a limited range of problems (strictly, where a one-to-one mapping exists between the initial and final particle distribution, since Eqs. 21–22 are essentially based on reconstructing the field at any time based on the initial conditions and the particle trajectories).

3) The vector potential and other disasters: Price [29] performed an extensive investigation of the vector potential $\mathbf{B} = \nabla\times\mathbf{A}$ as an alternative to the Euler potentials, containing similar preventative properties but with no restriction on the field geometry and allowing non-ideal MHD effects to be incorporated in a straightforward manner. The first problem with this approach is that the evolution equation for the vector potential in 3D is much more complicated than for the Euler potentials, given, with an appropriate choice of gauge, by

$$\begin{aligned} \frac{d\mathbf{A}}{dt} &= -\mathbf{A}\times(\nabla\times\mathbf{v}) - (\mathbf{A}\cdot\nabla)\mathbf{v}, \\ &= -A^j\nabla v^j. \end{aligned} \tag{23}$$

While a simple approach is simply to discretise this equation, solve $\mathbf{B} = \nabla\times\mathbf{A}$ and use the resulting $\mathbf{B}$ in the standard SPMHD equations, this was found by [29] to contain an instability related to the evolution of $\mathbf{A}$ (though the origin was not fully understood). Also, the source term approach should be unnecessary since the divergence constraint should be somehow 'built-in' to the equations. For this reason, [29] derived a self-consistent formulation of the vector-potential based SPMHD equations from a variational principle, where one uses the discrete operator for the curl and the discrete representation of Eq. 23 to *derive* the discrete equations of motion.

With the curl constructed using the differenced curl operator, i.e.

$$\mathbf{B}_a = (\nabla\times\mathbf{A})_a = \frac{1}{\rho_a}\sum_b m_b(\mathbf{A}_a - \mathbf{A}_b)\times\nabla_a W_{ab}, \tag{24}$$

and with similar operators used to discretise Eq. 23, the resultant equations of motion are given by

$$\begin{aligned} \frac{d\mathbf{v}_a}{dt} &= -\sum_b m_b\left(\frac{P_a - \frac{3}{2\mu_0}B_a^2}{\rho_a^2} + \frac{P_b - \frac{3}{2\mu_0}B_b^2}{\rho_b^2}\right)\nabla_a W_{ab} \\ &- \frac{1}{\mu_0}\sum_b m_b\left\{\left(\frac{\mathbf{B}_a}{\rho_a^2} + \frac{\mathbf{B}_b}{\rho_b^2}\right)\cdot[(\mathbf{A}_a - \mathbf{A}_b)\times\nabla]\right\}\nabla_a W_{ab} \\ &- \sum_b m_b\left[\frac{\mathbf{A}_a}{\rho_a^2}\mathbf{J}_a\cdot\nabla_a W_{ab} + \frac{\mathbf{A}_b}{\rho_b^2}\mathbf{J}_b\cdot\nabla_a W_{ab}\right], \end{aligned} \tag{25}$$

where $\mathbf{J}$ is the magnetic current computed using the symmetric curl operator (the conjugate to 24),

$$\mathbf{J}_a \equiv \frac{(\nabla\times\mathbf{B})_a}{\mu_0} \equiv -\frac{\rho_a}{\mu_0}\sum_b m_b\left[\frac{\mathbf{B}_a}{\rho_a^2} + \frac{\mathbf{B}_b}{\rho_b^2}\right]\times\nabla_a W_{ab}. \tag{26}$$

These equations are remarkable in showing that it is possible to self-consistently derive SPMHD equations even in this quite complicated case, and revealing the symmetry between the differencing and symmetric operators in SPH, since the symmetric operator in Eq. 26 directly follows from having employed the differencing operator in Eq. 24. This is similar to the usual SPH equations, where the appearance of the differencing operator for $\nabla\cdot\mathbf{v}$ in the continuity equation (i.e., taking the time derivative of Eq. 5) directly leads to the symmetric operator for the pressure gradient in the equations of motion (Eq. 6).

Unfortunately, Eq. 25 was found to be highly unstable to the tensile instability as soon as $\frac{3}{2}B^2/\mu_0 > P$, a much harsher criterion than for the usual SPMHD equations, and one that proves difficult to stabilise. Thus [29] concluded that the vector potential was not a viable approach to SPMHD.

4) Cleaning revisited: Meanwhile, Florian Bürzle and colleagues [6], [7] found that simply using the standard SPMHD equations Eqs. 5–7 with source term correction (Eq. 9) and artificial resistivity (Eq. 13) could be sufficient for even quite complicated problems (including the formation of stars from magnetised clouds), in effect using the artificial resistivity to control the divergence errors. However, the divergence errors remain uncomfortably high (of order unity or higher) and can

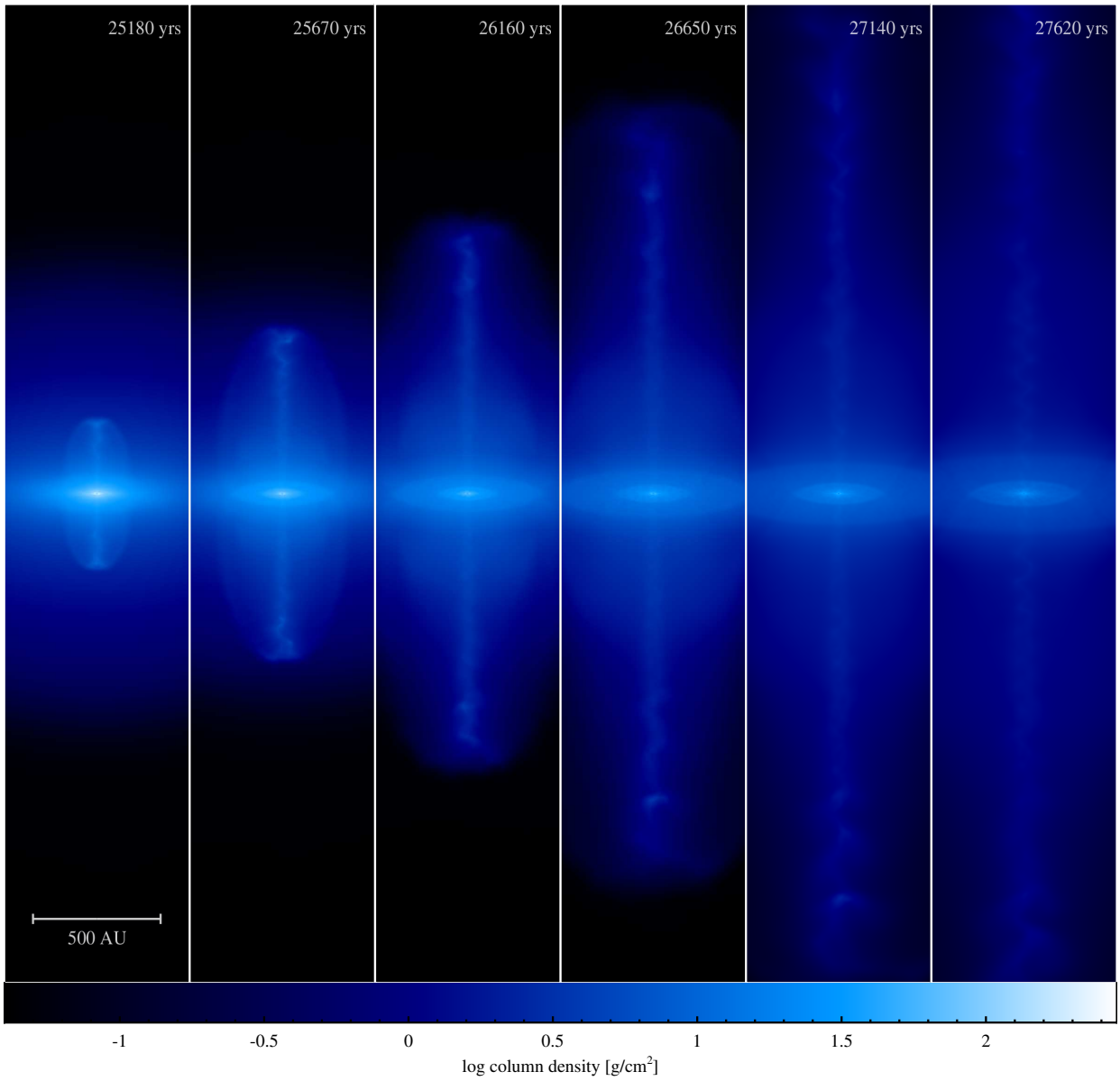

Fig. 1. Star formation simulation, showing the gravitational collapse of a magnetised, rotating gas cloud to form a protostar. As the collapse proceeds, the magnetic field is wound up by the flow and a 'jet' of gas is launched at high speed (2–7 km/s). This is the first time we have been able to simulate such complicated magnetic phenomena with Smoothed Particle Magnetohydrodynamics, made possible by our recent development of a robust method for cleaning divergence errors associated with the magnetic field.

still present a problem in highly dynamic regions. This, and the tragic experience of the vector potential, motivated us to revisit the formulation of hyperbolic/parabolic cleaning by [8], found to be rather ineffective and somewhat dangerous by [38], since it could lead under some circumstances to growth rather than decay of divergence errors. In this scheme, an additional term is added to the MHD induction equation given by

$$\left(\frac{\mathrm{d}\mathbf{B}}{\mathrm{d}t}\right)_{clean} = -\nabla\psi, \tag{27}$$

where ψ is a new scalar field that is evolved according to

$$\frac{\mathrm{d}\psi}{\mathrm{d}t} = c_h^2(\nabla\cdot\mathbf{B}) - \frac{\psi}{\tau}, \tag{28}$$

which combine to produce a damped wave equation for ψ (or equivalently $\nabla\cdot\mathbf{B}$),

$$\frac{1}{c_h^2}\frac{\partial^2\psi}{\partial t^2} - \nabla^2\psi + \frac{1}{c_h^2\tau}\frac{\partial\psi}{\partial t} = 0, \tag{29}$$

meaning that divergence errors will both be propagated in a wavelike manner at speed c_h (typically chosen to be the

maximum speed allowed by the timestep constraint) and decay on a timescale τ (chosen to balance spreading and cleaning in some appropriate manner).

Although the details can be found in Tricco (this proceedings) and in [43], the key idea we employed was to formulate the cleaning equations Eqs. 27–28 in a conservative manner. This was found to require use of conjugate SPH operators in the discrete formulation of the cleaning equations, i.e. if the differencing operator was used to represent $\nabla\cdot\mathbf{B}$ in Eq. 28 then the symmetric operator was found to be required for $\nabla\psi$ in Eq. 27. With this constraint, and with an appropriate choice of decay timescale, the cleaning was found to be both safe and effective, effectively solving the divergence problem in SPMHD in a very simple way. Furthermore, applying this cleaning was found to improve momentum conservation by two orders of magnitude compared to the artificial-resistivity-only approach on one of the main problems of interest, involving the launch of protostellar jets [43].

F. Protostellar jets with SPMHD

A spectacular demonstration of our newfound ability to robustly simulate complicated magnetic phenomena by adopting the new cleaning scheme in SPMHD was given by [40], modelling the collapse of a magnetised, rotating gas cloud in a preliminary stage of star formation (that is, to the formation of the 'first core', an initial stall phase during the formation of a protostar). The results of the calculation, showing the integrated density along the line of sight, are shown in Fig. 1, and clearly demonstrate the launching of a 'jet' of gas due to the winding up of the magnetic field in the rotating, collapsing flow. This is the first time that we have been able to reproduce such phenomena with SPMHD simulations, despite collimated jets and outflows being widely observed in nature, and opens the door to a huge range of future possibilities. Thus, after 35 years of trying, it seems we finally have a robust and general approach to solving the equations of MHD in SPH.

III. Turbulence

Modelling turbulence is also of key importance for star formation, since motions in the molecular clouds from which stars are born are observed to exceed the speed of sound in these clouds with Mach numbers of up to 20 on the largest scales. Furthermore, the statistics of the supersonic, weakly magnetised (super-Alfvénic) turbulence is thought to determine, amongst other things, the eventual mass distribution of stars, the morphology of interstellar clouds and perhaps even the star formation rate (see review by [17]). Thus, in astrophysics the main interest is in understanding turbulence at high Mach number, which has received relatively little attention theoretically and is difficult to address with laboratory experiments on Earth. Furthermore, Reynolds numbers in the interstellar medium are estimated to be $\sim 10^5$–10^6 [9], meaning that direct numerical simulations that resolve the dissipation scale are as beyond the reach of current computational power.

A. Supersonic turbulence with SPH

Many of the early numerical studies of turbulence in the interstellar medium (e.g. [1], [12], [45]) used SPH, mainly because of the ease with which studies that include self-gravity could be performed. However, these simulations employed a relatively low resolution ($\sim 200,000$ particles in 3D, c.f. [1], [45]), making it difficult to make definitive statements regarding statistical properties of turbulence such as the power spectra or Probability Density Functions (PDFs). With the advent of high resolution grid-based simulations of supersonic, isothermal turbulence at 1024^3 and beyond [14] (without self-gravity), the SPH studies came in for some criticism. For example [24], commenting on the non-self-gravitating simulations of [1], wrote that

> "The complete absence of an inertial range with a reasonable slope, or with a reasonable dependence of the slope on the Mach number, makes their SPH simulations totally inadequate for testing the turbulent fragmentation model".

Their criticism was based mainly on comparing the kinetic energy power spectra obtained in the SPH calculations with those of the grid based calculations performed by [24], where it was found that the SPH calculations produced much steeper power spectra than the grid-based codes ($P(k) \propto k^{-\beta}$ where $\beta = 2.7$–2.9 was found from the SPH results compared to 2.0–2.2 in the grid based results).

B. Simulating turbulence at high resolution in SPH

Since it seemed that the main limitation in the SPH calculations was simply the numerical resolution employed (though this was by no means clear in the debate between the above authors), the key element was to develop a new SPH code, PHANTOM, designed to run this kind of problem efficiently and at high resolution [15], [34]. The main design choices in developing PHANTOM were to:

1) Use a simple fixed-grid neighbour finding scheme in place of a treecode for these kind of problems
2) Rewrite the basic SPH algorithm so that it can be performed with one global loop over the particles
3) Use a cache of trial neighbour positions and neighbour lists, shared between all particles in a cell

Implementing (2) simply involves a slight modification to the artificial viscosity terms, such that the SPH equations of motion could be written in the form

$$\frac{\mathrm{d}\mathbf{v}_a}{\mathrm{d}t} = \sum_b m_b \left[\frac{P_a + q_a}{\Omega_a \rho_a^2} \frac{\partial W_{ab}(h_a)}{\partial \mathbf{r}_a} + \frac{P_b + q_b}{\Omega_b \rho_b^2} \frac{\partial W_{ab}(h_b)}{\partial \mathbf{r}_a} \right], \tag{30}$$

where q_a is the artificial viscosity between the pair using the density and other quantities evaluated at particle a, given by

$$q_a = \begin{cases} \frac{1}{2}\alpha_a \rho_a v_{sig,a} |\mathbf{v}_{ab}\cdot\hat{\mathbf{r}}_{ab}|, & \mathbf{v}_{ab}\cdot\hat{\mathbf{r}}_{ab} < 0 \\ 0 & \mathbf{v}_{ab}\cdot\hat{\mathbf{r}}_{ab} \geq 0 \end{cases} \tag{31}$$

where $\mathbf{v}_{ab} \equiv \mathbf{v}_a - \mathbf{v}_b$ and the signal velocity at a is given by

$$v_{sig,a} = c_{s,a} + \beta_{visc} |\mathbf{v}_{ab}\cdot\hat{\mathbf{r}}_{ab}| \tag{32}$$

with the corresponding expressions at particle b. This is essentially the same as the formulation of artificial viscosity given in [18] but with a different symmetrisation of the density and signal velocity terms.

With this minor modification to the SPH algorithm, it is possible to compute the density and equations of motion in a single, global loop over the particles (but with several loops over the neighbour list for each particle). This proceeds as follows:

1) The loop proceeds over all grid cells or 'nodes', finding and caching a shared trial neighbour list for each cell
2) For each particle in the cell, the density is calculated on a particle a by finding all neighbours within h_a (c.f. Eq. 5). This may need to be iterated several times in order to solve for h_a and ρ_a self-consistently (c.f. [39]) but this is computationally efficient since since the neighbour list can be cached and re-used while setting h (to avoid multiple neighbour finds when h increases one can simply search to a slightly larger radius than strictly necessary in the first instance).
3) Using the same neighbour list, the first term in Eq. 30 (involving P_a/ρ_a^2) can be computed, with the force term simultaneously *given* to all neighbouring particles, thus incrementally computing the second term in Eq. 30 on the neighbours.

The advantage of the above is that only one neighbour finding procedure is invoked, which is the key bottleneck in most SPH codes. Also, parallelisation is relatively straightforward, since it simply involves splitting the main loop into chunks to be handled by each processor.

With the algorithm above, PHANTOM was benchmarked to around an order of magnitude faster than standard tree-based SPH codes for turbulence problems [11], thus solving one of the main issues with studying turbulence using SPH.

C. A comparison between SPH and grid-based methods on driven, supersonic, isothermal turbulence

In [34] we set out to perform a detailed comparison study between SPH (using PHANTOM) and a grid-based code (FLASH) on the statistics of supersonic, isothermal turbulence, driven artificially in Fourier space and supplying energy continuously on large scales, such that a statistical steady state would develop. The advantage of performing a comparison of driven turbulence is that the initial conditions are completely trivial for both codes, unlike for decaying turbulence where it is necessary to start from a pre-evolved initial condition computed with one of the codes [11]. The comparison involved performing calculations at 3 different resolutions, 128^3, 256^3 and 512^3 particles with both grid and SPH codes. Since the physical Reynolds numbers are high and supersonic turbulence is in any case dominated by shock dissipation rather than Navier-Stokes viscosity, the calculations were performed in both codes applying only shock viscosity (i.e., artificial rather than physical viscosity in SPH).

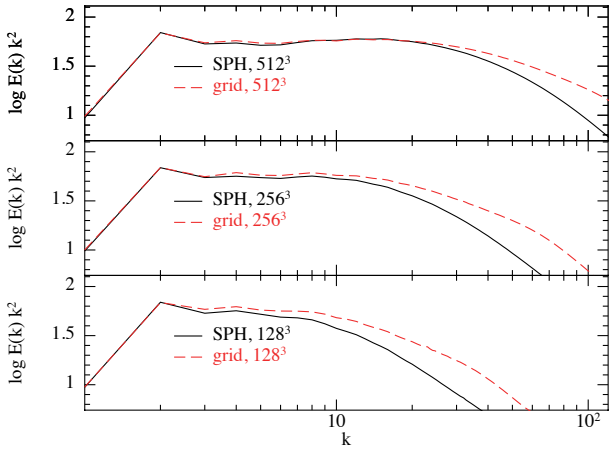

Fig. 2. Time-averaged kinetic energy power spectra, compensated by k^2, from a comparison between grid and SPH codes on the statistics of driven, supersonic, isothermal turbulence at Mach 10 [34]. For power spectra, similar results are obtained when the number of particles is similar to the number of grid cells.

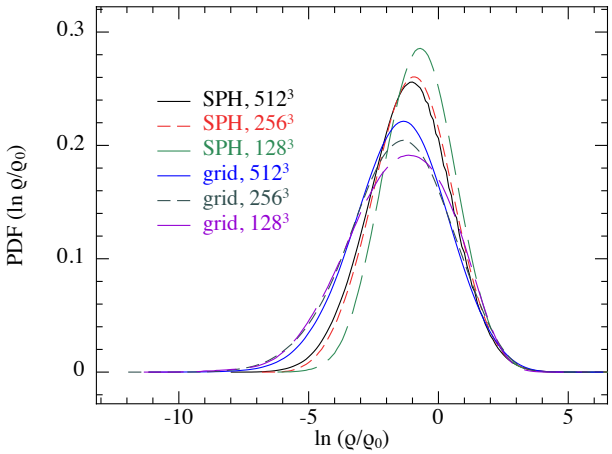

Fig. 3. Time-averaged density PDFs from the Mach 10 turbulence comparison. SPH obtains converged results in the PDF using $\gtrsim 256^3$ particles, resolving maximum densities at this resolution that would only be resolved by the grid code at this Mach number using $\gtrsim 1024^3$ grid cells.

The main outcome of the study in [34] was that, for volumetric quantities like the kinetic energy power spectrum, comparable results were obtained between codes when the number of particles is similar to the number of grid cells (Fig. 2). This indicated that, indeed, the disagreement between [1] and [24] was simply because the SPH calculations were performed at a much lower resolution than the grid-based simulations. In this respect, SPH is not the most efficient technique for studying power spectra, since even with PHANTOM the SPH simulations were around an order of magnitude slower than the grid simulations with $n_{part} = n_{cells}$.

The advantage of SPH, however, is that the resolution is automatically placed in the density field. This means that the density PDF is much better sampled with SPH than with a grid-based code, particularly at the high density end which is

most relevant to star formation. In particular, the maximum density resolved by SPH using 128^3 particles was found to be similar to that resolved by the grid using 512^3 grid cells, and the time-averaged PDF is converged in SPH using $\gtrsim 256^3$ particles but remains unconverged in the grid code even at 512^3 (Fig. 3), implying that for studying the PDF that SPH is around an order of magnitude more efficient in terms of computational cost. This means that SPH is a useful tool for studying the statistics of the density field in supersonic turbulence, e.g. studying the relationship between the density variance and the Mach number in supersonic flow that is assumed in several analytic star formation models [35].

D. SPH—grid comparisons at low Mach number

For subsonic flow no equivalent comparison has been performed, although recent work in 2D has compared SPH results to both analytic theory and experimental results [21], [44]. To this end [2] attempted (unsuccessfully) to extend the comparison performed in [34] to the subsonic regime. However, they found strong disagreement in the subsonic regime, finding that the SPH power spectra showed essentially no power-law inertial range and were far too steep even at low k, implying that "SPH fails quite badly in the subsonic regime". In the initial preprint posted on the arXiv server this was attributed to "large errors in SPH's gradient estimate and associated subsonic velocity noise". The fatal flaw in their initial study, pointed out in a refereed response [30] (that, somewhat backwardly, appeared in print before the final version of the paper itself) was that no attempt was made to control the viscosity in their SPH calculations, simply using a standard artificial viscosity with $\alpha = 1$. Worse still, for a comparison of subsonic turbulence, the initial preprint contained no mention whatsoever of the Reynolds number, neither to estimate it nor fix its value, somewhat critical in the subsonic regime since it is the main dimensionless parameter characterising the flow.

It is straightforward to estimate the Reynolds number in SPH calculations, since the artificial viscosity terms can be directly translated into their physical equivalents, giving a shear and bulk viscosities coefficients of (e.g. [15], [20])

$$\nu \approx \frac{1}{10}\alpha v_{\rm sig} h; \qquad \zeta \approx \frac{1}{6}\alpha v_{\rm sig} h, \tag{33}$$

where α is the artificial viscosity parameter and $v_{\rm sig}$ is the signal velocity used in the artificial viscosity term. The corresponding Reynolds number is thus given by

$$\mathcal{R}_{\rm e} \equiv \frac{VL}{\nu} = \frac{10}{\alpha}\mathcal{M}\frac{L}{h}, \tag{34}$$

where M is the Mach number, L/h is the ratio of the box size to the smoothing length and d is the number of spatial dimensions.

It is easy to show that naively employing $\alpha = 1$ will lead to very low Reynolds numbers in the subsonic regime even at high resolution (Eq. 34 gives $R_e \approx 600$ with 256^3 particles at the Mach number employed by [2]). The result is that one *should not expect* an inertial range at such low Reynolds numbers. Fortunately it is straightforward to reduce the viscosity since there are no strong shocks in the calculations. Thus [30] demonstrates that a Kolmogorov-like spectrum is easily recoverable by simply using standard viscosity switches [23] (Fig. 4). Nevertheless, in the published version of their paper, responding in turn to [30], the authors maintain their argument that SPH is still somehow fundamentally flawed, despite the fact that, once the Reynolds number is sufficiently high, a Kolmogorov-spectrum *can* clearly be reproduced in spite of such 'fundamental' difficulties. The argument is yet to be resolved.

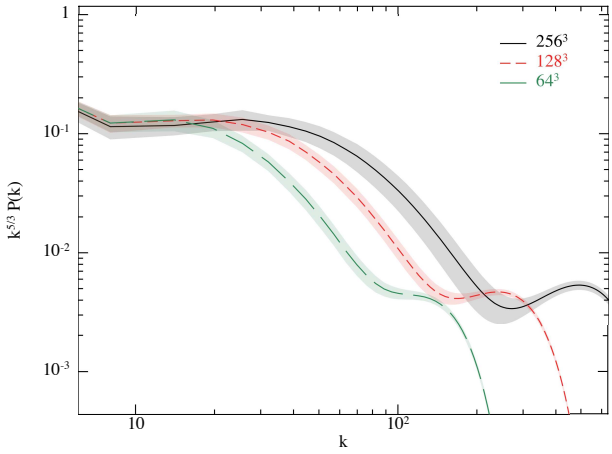

Fig. 4. Time-averaged kinetic energy power spectra (compensated by $k^{5/3}$) in calculations of subsonic ($M \approx 0.3$) isothermal, compressible turbulence, computed using SPH at 3 different resolutions using a viscosity switch to obtain higher Reynolds numbers than in the [2] calculations. A small inertial range with a Kolmogorov $k^{-5/3}$ slope is clearly evident (horizontal in this figure). See [30].

IV. Conclusion

In summary, we have recently made key advances in modelling both magnetic fields and turbulence in SPH. For magnetic fields, the most important advance is the recent development of a robust divergence cleaning algorithm for SPMHD [43], enabling for the first time simulations of complex magnetically-driven phenomena such as the launch of collimated jets during the formation of stars. In modelling turbulence, the most important aspects appear to be employing a high numerical resolution (current simulations employ up to 512^3 particles) together with viscosity switches in order to reach sufficiently high Reynolds numbers that a scale-free inertial range can develop.

Acknowledgment

DJP would like to thank Joe Monaghan for getting me into this game in the first place. Figures have been produced with SPLASH [28], a publicly available visualisation tool for SPH available from http://users.monash.edu.au/~dprice/splash/.

REFERENCES

[1] Ballesteros-Paredes, J., A. Gazol, J. Kim, R. S. Klessen, A.-K. Jappsen, and E. Tejero: 2006, 'The Mass Spectra of Cores in Turbulent Molecular Clouds and Implications for the Initial Mass Function'. *ApJ* **637**, 384–391.

[2] Bauer, A. and V. Springel: 2011, 'Subsonic turbulence in smoothed particle hydrodynamics and moving-mesh simulations'. *MNRAS, in press*.

[3] Børve, S., M. Omang, and J. Trulsen: 2001, 'Regularized Smoothed Particle Hydrodynamics: A New Approach to Simulating Magnetohydrodynamic Shocks'. *ApJ* **561**, 82–93.

[4] Børve, S., M. Omang, and J. Trulsen: 2006, 'Multidimensional MHD Shock Tests of Regularized Smoothed Particle Hydrodynamics'. *ApJ* **652**, 1306–1317.

[5] Brandenburg, A.: 2010, 'Magnetic field evolution in simulations with Euler potentials'. *MNRAS* **401**, 347–354.

[6] Bürzle, F., P. C. Clark, F. Stasyszyn, K. Dolag, and R. S. Klessen: 2011a, 'Protostellar outflows with smoothed particle magnetohydrodynamics'. *MNRAS* **417**, L61–L65.

[7] Bürzle, F., P. C. Clark, F. Stasyszyn, T. Greif, K. Dolag, R. S. Klessen, and P. Nielaba: 2011b, 'Protostellar collapse and fragmentation using an MHD GADGET'. *MNRAS* **412**, 171–186.

[8] Dedner, A., F. Kemm, D. Kröner, C.-D. Munz, T. Schnitzer, and M. Wesenberg: 2002, 'Hyperbolic Divergence Cleaning for the MHD Equations'. *J. Comp. Phys.* **175**, 645–673.

[9] Elmegreen, B. G. and J. Scalo: 2004, 'Interstellar Turbulence I: Observations and Processes'. *ARA&A* **42**, 211–273.

[10] Gingold, R. A. and J. J. Monaghan: 1977, 'Smoothed particle hydrodynamics - Theory and application to non-spherical stars'. *MNRAS* **181**, 375–389.

[11] Kitsionas, S., C. Federrath, R. S. Klessen, W. Schmidt, D. J. Price, L. J. Dursi, M. Gritschneder, S. Walch, R. Piontek, J. Kim, A. Jappsen, P. Ciecielag, and M. Mac Low: 2009, 'Algorithmic comparisons of decaying, isothermal, supersonic turbulence'. *A&A* **508**, 541–560.

[12] Klessen, R. S., F. Heitsch, and M.-M. Mac Low: 2000, 'Gravitational Collapse in Turbulent Molecular Clouds. I. Gasdynamical Turbulence'. *ApJ* **535**, 887–906.

[13] Kotarba, H., H. Lesch, K. Dolag, T. Naab, P. H. Johansson, and F. A. Stasyszyn: 2009, 'Magnetic field structure due to the global velocity field in spiral galaxies'. *MNRAS* **397**, 733–747.

[14] Kritsuk, A. G., M. L. Norman, P. Padoan, and R. Wagner: 2007, 'The Statistics of Supersonic Isothermal Turbulence'. *ApJ* **665**, 416–431.

[15] Lodato, G. and D. J. Price: 2010, 'On the diffusive propagation of warps in thin accretion discs'. *MNRAS* **405**, 1212–1226.

[16] Lucy, L. B.: 1977, 'A numerical approach to the testing of the fission hypothesis'. *Astron. J.* **82**, 1013–1024.

[17] Mac Low, M. and R. S. Klessen: 2004, 'Control of star formation by supersonic turbulence'. *Rev. Mod. Phys.* **76**, 125–194.

[18] Monaghan, J. J.: 1997, 'SPH and Riemann Solvers'. *J. Comp. Phys.* **136**, 298–307.

[19] Monaghan, J. J.: 2002, 'SPH compressible turbulence'. *MNRAS* **335**, 843–852.

[20] Monaghan, J. J.: 2005, 'Smoothed particle hydrodynamics'. *Rep. Prog. Phys.* **68**(8), 1703–1759.

[21] Monaghan, J. J.: 2011, 'A turbulence model for Smoothed Particle Hydrodynamics'. *Eur. J. Mech. B/Fluids* **30**, 360–370.

[22] Morris, J. P.: 1996, 'Analysis of smoothed particle hydrodynamics with applications'. Ph.D. thesis, Monash University, Melbourne, Australia.

[23] Morris, J. P. and J. J. Monaghan: 1997, 'A switch to reduce SPH viscosity'. *J. Comp. Phys.* **136**, 41–50.

[24] Padoan, P., Å. Nordlund, A. G. Kritsuk, M. L. Norman, and P. S. Li: 2007, 'Two Regimes of Turbulent Fragmentation and the Stellar Initial Mass Function from Primordial to Present-Day Star Formation'. *ApJ* **661**, 972–981.

[25] Phillips, G. J. and J. J. Monaghan: 1985, 'A numerical method for three-dimensional simulations of collapsing, isothermal, magnetic gas clouds'. *MNRAS* **216**, 883–895.

[26] Powell, K. G., P. L. Roe, T. J. Linde, T. I. Gombosi, and D. L. de Zeeuw: 1999, 'A Solution-Adaptive Upwind Scheme for Ideal Magnetohydrodynamics'. *J. Comp. Phys.* **154**, 284–309.

[27] Price, D. J.: 2004, 'Magnetic fields in Astrophysics'. Ph.D. thesis, University of Cambridge, Cambridge, UK. astro-ph/0507472.

[28] Price, D. J.: 2007, 'SPLASH: An Interactive Visualisation Tool for Smoothed Particle Hydrodynamics Simulations'. *Publ. Astron. Soc. Aust.* **24**, 159–173.

[29] Price, D. J.: 2010, 'Smoothed Particle Magnetohydrodynamics - IV. Using the vector potential'. *MNRAS* **401**, 1475–1499.

[30] Price, D. J.: 2012a, 'Resolving high Reynolds numbers in smoothed particle hydrodynamics simulations of subsonic turbulence'. *MNRAS* **420**, L33–L37.

[31] Price, D. J.: 2012b, 'Smoothed Particle Hydrodynamics and Magnetohydrodynamics'. *J. Comp. Phys.* **231**, 759–794.

[32] Price, D. J. and M. R. Bate: 2007, 'The impact of magnetic fields on single and binary star formation'. *MNRAS* **377**, 77–90.

[33] Price, D. J. and M. R. Bate: 2008, 'The effect of magnetic fields on star cluster formation'. *MNRAS* **385**, 1820–1834.

[34] Price, D. J. and C. Federrath: 2010, 'A comparison between grid and particle methods on the statistics of driven, supersonic, isothermal turbulence'. *MNRAS* **406**, 1659–1674.

[35] Price, D. J., C. Federrath, and C. M. Brunt: 2011, 'The Density Variance–Mach Number Relation in Supersonic, Isothermal Turbulence'. *ApJL* **727**, L21.

[36] Price, D. J. and J. J. Monaghan: 2004a, 'Smoothed Particle Magnetohydrodynamics - I. Algorithm and tests in one dimension'. *MNRAS* **348**, 123–138.

[37] Price, D. J. and J. J. Monaghan: 2004b, 'Smoothed Particle Magnetohydrodynamics - II. Variational principles and variable smoothing-length terms'. *MNRAS* **348**, 139–152.

[38] Price, D. J. and J. J. Monaghan: 2005, 'Smoothed Particle Magnetohydrodynamics - III. Multidimensional tests and the $\nabla \cdot \mathbf{B} = 0$ constraint'. *MNRAS* **364**, 384–406.

[39] Price, D. J. and J. J. Monaghan: 2007, 'An energy-conserving formalism for adaptive gravitational force softening in smoothed particle hydrodynamics and N-body codes'. *MNRAS* **374**, 1347–1358.

[40] Price, D. J., T. S. Tricco, and M. R. Bate: 2012, 'Collimated jets from the first core'. *MNRAS Letters, submitted*.

[41] Rosswog, S. and D. Price: 2007, 'MAGMA: a three-dimensional, Lagrangian magnetohydrodynamics code for merger applications'. *MNRAS* **379**, 915–931.

[42] Stern, D. P.: 1966, 'The Motion of Magnetic Field Lines'. *Space Science Reviews* **6**, 147.

[43] Tricco, T. S. and D. J. Price: 2012, 'Constrained hyperbolic divergence cleaning for Smoothed Particle Magnetohydrodynamics'. *submitted to J. Comp. Phys.*

[44] Valizadeh, A. and J. J. Monaghan: 2012, 'Smoothed particle hydrodynamics simulations of turbulence in fixed and rotating boxes in two dimensions with no-slip boundaries'. *Physics of Fluids* **24**(3), 035107.

[45] Vázquez-Semadeni, E., J. Ballesteros-Paredes, and R. S. Klessen: 2003, 'A Holistic Scenario of Turbulent Molecular Cloud Evolution and Control of the Star Formation Efficiency: First Tests'. *ApJL* **585**, L131–L134.